

Heisenberg-limited metrology from the quantum-quench dynamics of an anisotropic ferromagnet

Z. M. McIntyre,* Ji Zou,† Jelena Klinovaja, and Daniel Loss

Department of Physics, University of Basel, Klingelbergstrasse 82, 4056 Basel, Switzerland

(Dated: December 30, 2025)

The emerging field of quantum magnonics seeks to understand and harness the quantum properties of magnons—quantized collective spin excitations in magnets. Squeezed magnon states arise naturally as the equilibrium ground states of anisotropic ferromagnets and antiferromagnets, representing an important class of nonclassical magnon states. In this work, we show how a qubit-conditioned quantum quench of an anisotropic ferromagnet can be used for Heisenberg-limited parameter estimation based on measurements of the qubit only. In the presence of ground-state squeezing, the protocol yields information about the eigenmode frequency of the coupled magnon-qubit system, whereas no information is gained in the absence of such squeezing. The protocol therefore leverages genuine quantum correlations in the form of magnonic squeezing while simultaneously relying on the equilibrium character of this squeezing—a feature distinctive to magnetic systems.

Introduction—Understanding, manipulating, and harnessing the quantum properties of bosonic excitations is central to modern quantum science, spanning a wide range of platforms ranging from optical [1] and mechanical [2] to magnetic systems [3]. The quantum nature of magnons, the quanta of collective spin excitations in magnets, has attracted intense interest in recent years, giving rise to the emerging and rapidly developing field of *quantum magnonics*, see Refs. [3, 4] for reviews. Magnons hold promise as information carriers in quantum networks [5], and significant progress has been made—not only theoretically but experimentally as well—towards the coherent control and measurement of quantum magnonic states via qubits [6–10].

Among nonclassical states, squeezed states [11] stand out for their reduced quantum fluctuations along one quadrature, allowing for more precise measurements of unknown parameters in the context of quantum metrology. The maximum precision that can be achieved in estimating an unknown parameter ϕ using separable N -particle states is given by the standard quantum limit (SQL), $\delta\phi = 1/\sqrt{NM}$ with M giving the number of independent measurements [12]. The fundamental goal of quantum metrology is to estimate ϕ from measurements of a quantum state with a precision scaling like $N^{-\nu}$ with $\nu > 1/2$, outperforming the SQL. For a state having a fixed number N of particles, the best achievable precision is given by the Heisenberg limit, $\delta\phi = 1/(N\sqrt{M})$ [12]. The benefits of using squeezed vacuum states for quantum metrology has been widely studied and demonstrated in the context of interferometry with quantum states of light [13–16]. Most famously, squeezed vacuum has been used by LIGO to enhance the sensitivity of gravitational wave detection [17]. Squeezed spin states of atomic ensembles [18] can also be used for quantum-enhanced precision in atomic Ramsey interferometry [19–21]. In this case, the precision gain for N spins relative to the SQL is captured by a spin-squeezing parameter $\xi < 1$ scaling like some power of $1/N$, in terms of which

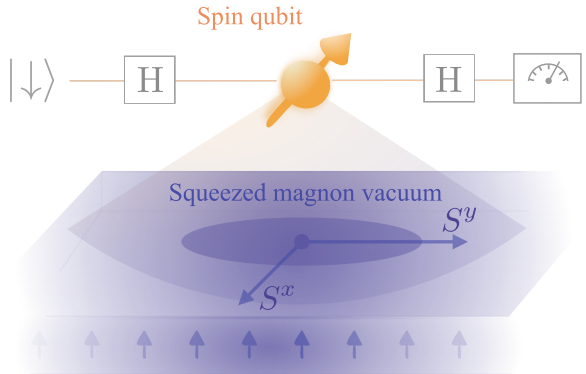


FIG. 1. Schematic of a spin qubit coupled to the Kittel mode of an anisotropic ferromagnet. The ground state of the Kittel mode is a squeezed state whose reduced quantum fluctuations along one quadrature can be harnessed through the qubit for Heisenberg-limited parameter estimation.

$\delta\phi = \xi/\sqrt{NM}$ [19]. For squeezing generated via one-axis twisting, for instance, ξ scales like $N^{-1/3}$ for large N [22, 23].

Squeezed light and spin-squeezed atomic ensembles are both typically generated dynamically using strategies like Feshbach-resonance-induced interactions [23], cavity-mediated interactions [24], and parametric down-conversion [25]. In stark contrast, squeezed magnonic states exist ubiquitously in nature, being found for instance in anisotropic ferromagnets [26–28] and antiferromagnets [29]. In these systems, squeezing emerges as an intrinsic feature of the magnetic ground state proceeding from energy minimization [30]. Despite growing theoretical understanding and recent proposals for detecting such states [31, 32], this equilibrium origin makes it challenging to access and harness magnon squeezing for useful applications. A key impediment to leveraging magnon squeezing for quantum metrology is the development of concrete measurement strategies enabling sub-SQL parameter estimation. For interferometry with pho-

tonic states, number-resolving measurements [14, 15, 33], parity measurements [34, 35], and homodyne detection [36, 37] can all be implemented using existing technologies. For atomic interferometers, the required atomic population measurements have been realized [21], and the atomic analog of homodyne detection has been demonstrated experimentally as well [38].

In this work, we show how a qubit-conditioned quantum quench of the magnon mode could be used for Heisenberg-limited estimation of an unknown frequency based on measurements of the qubit. Such measurements have been realized for qubits coupled to magnons [6–9]. Conditioned on the qubit state, the quench will create real, squeezed magnons out of the Bogoliubov vacuum in a process similar to the dynamical Casimir effect [39]. Under free evolution, the interaction of the qubit with these squeezed magnons will lead to super-resolution [40] of the unknown parameter in the qubit coherence, enabling Heisenberg-limited parameter estimation via X-basis qubit readout. Crucially, no information about the unknown parameter is obtained in the absence of ground-state (equilibrium) squeezing of the magnon mode. This protocol therefore harnesses not only quantum effects in the form of squeezing, but also the equilibrium nature of this squeezing.

Model—We consider an anisotropic ferromagnet exchange-coupled to a spin qubit (Fig. 1). The microscopic Hamiltonian H_{sys} describing this system (setting $\hbar = 1$) is $H_{\text{sys}} = \Delta \sigma_z/2 - J \sum_{\langle i,j \rangle} \mathbf{S}_i \cdot \mathbf{S}_j - K_z \sum_i (S_i^z)^2 - K_y \sum_i (S_i^y)^2 - |\gamma| \mu_0 h \sum_i S_i^z - J_{\text{int}} \sum_i \mathbf{S}_i \cdot \boldsymbol{\sigma}$. Here, Δ and $\sigma_z = |\uparrow\rangle\langle\uparrow| - |\downarrow\rangle\langle\downarrow|$ are the spin-qubit splitting and Pauli-Z operator, $J > 0$ denotes the ferromagnetic exchange coupling, and $K_z, K_y > 0$ represent easy-axis anisotropies along the z - and y -directions, respectively. The parameter h denotes an external magnetic field applied parallel to the z -axis ($\mathbf{h} = h\hat{z}$), $\gamma = -28$ GHz/T is a gyromagnetic ratio, μ_0 is the vacuum magnetic permeability, and J_{int} is the interfacial exchange coupling strength between the spin qubit and ferromagnet. We focus on the Kittel ($\mathbf{k} = 0$) mode of the magnet, described by the magnon creation operator m^\dagger , and we work in the detuned regime where the qubit is far off-resonant from the magnon frequency, allowing flip-flop terms in the exchange interaction to be neglected. In a frame rotating at the qubit splitting Δ , the effective Hamiltonian for the Kittel mode is then given by [31, 41]

$$H = H_0 + H_{\text{int}}, \quad (1)$$

where

$$H_0 = \omega_0 m^\dagger m + \Omega(m^2 + \text{h.c.}), \quad (2)$$

$$H_{\text{int}} = \chi m^\dagger m \sigma_z. \quad (3)$$

Here $\omega_0 = 2SK_z - SK_y + |\gamma|\mu_0 h$ is the magnon-mode frequency, which is tunable via the external field h , and

$\Omega = SK_y/2$ with S denoting the length of the spin. The dispersive coupling strength χ appearing in Eq. (3) originates from the Ising term in the exchange interaction (and therefore does not fall off with detuning) and is given by $\chi = J_{\text{int}} N_{\text{int}} |\psi|^2 / (2N_F)$, where N_{int} is the number of interfacial spins, N_F is the total number of sites in the ferromagnet, and $|\psi|^2$ is the electronic wavefunction of the qubit averaged over the interface [31, 41]. Although Eqs. (2)-(3) were derived starting from a microscopic model H_{sys} in which the coupling between the (spin) qubit and the ferromagnetic spins originates from the exchange interaction, a dispersive coupling $m^\dagger m \sigma_z$ can also be realized for superconducting qubits by coupling both the superconducting qubit and Kittel mode to a microwave cavity mode [7, 8, 10].

The $U(1)$ -symmetry-breaking term $\Omega(m^2 + \text{h.c.})$ violates magnon-number conservation and changes the nature of the magnetic ground state: Instead of the vacuum Fock state $|0\rangle$ (defined by $m|0\rangle = 0$), the ground state of H is given by a nonclassical superposition of even-parity magnon states known as a squeezed magnon vacuum. To be exact, the ground state $|0\rangle_\sigma$ ($\sigma = \uparrow, \downarrow$) of H depends on the state $|\sigma\rangle$ of the qubit and is given by $|0\rangle_\sigma = S(r_\sigma)|0\rangle$, where $S(z) = \exp\{(z^* m^2 - \text{h.c.})/2\}$ is a squeezing operator acting on the magnon mode m . The strength r_σ of the squeezing is qubit-state-dependent and given by $r_\sigma = (1/2)\text{arctanh}[2\Omega/\omega_{\text{eff},\sigma}]$ with $\omega_{\text{eff},\uparrow} = \omega_0 + \chi$ and $\omega_{\text{eff},\downarrow} = \omega_0 - \chi$. Beyond the vacuum $|0\rangle_\sigma$, a similar relation also applies to arbitrary Fock states of H :

$$|n\rangle_\sigma = S(r_\sigma)|n\rangle. \quad (4)$$

We diagonalize the qubit-state-dependent magnon Hamiltonian $H_\sigma = \langle\sigma|H|\sigma\rangle$ via a Bogoliubov transformation, giving $H_\sigma = \omega_\sigma \alpha_\sigma^\dagger \alpha_\sigma$ with $\alpha_\sigma = S(r_\sigma) m S^\dagger(r_\sigma)$ and $\omega_\sigma = [\omega_{\text{eff},\sigma}^2 - 4\Omega^2]^{1/2}$. The magnetic system is stable when $\omega_{\text{eff},\sigma}^2 > 4\Omega^2$ for both σ . In terms of the Fock states $|n\rangle$ of the magnon mode m , the ground state $|0\rangle_\sigma$ is given by $|0\rangle_\sigma = \sum_n \langle n|S(r_\sigma)|0\rangle|n\rangle$. Using Eq. (4) to write $|n\rangle$ in the α_σ eigenbasis (i.e. $|n\rangle = \sum_m \langle m|S^\dagger(r_\sigma)|n\rangle|m\rangle_\sigma$ with $\uparrow = \downarrow$), it may then be seen that the ground state of the α_σ mode is a squeezed state of the α_σ mode with squeezing parameter $z_\sigma = r e^{i\theta_\sigma}$, where $r = r_\downarrow - r_\uparrow > 0$ and $\theta_\downarrow = 0$ and $\theta_\uparrow = \pi$ [31]:

$$|0\rangle_\sigma = \sum_{n=0}^{\infty} c_{2n}(z_\sigma) |2n\rangle_\sigma, \quad (5)$$

where $c_{2n}(z_\sigma) = \langle 2n|S(z_\sigma)|0\rangle$ are Fock-basis matrix elements of the squeezing operator [42]. We stress that the squeezing strength r is tunable via the magnon frequency ω_0 , controllable by an external magnetic field. We neglect magnon nonlinear effects, which is justified when $\sinh^2 r_\sigma \ll NS$, with N the total number of spins in the magnet. Consequently, the relative squeezing r is constrained by $\sinh^2 r = (2\chi/\Omega)^2 \sinh^2 r_\downarrow \sinh^2 r_\uparrow \ll (NS\chi/\Omega)^2$.

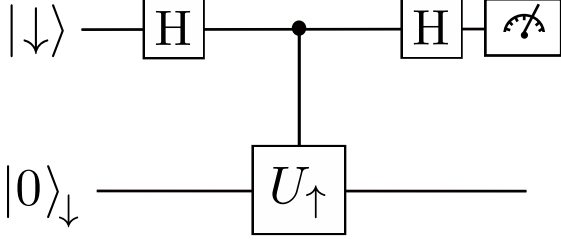


FIG. 2. Protocol expressed as a circuit. The magnon mode is allowed to equilibrate while in contact with the qubit held in $|\downarrow\rangle$. The squeezed magnons used for parameter estimation are produced by subjecting the magnon system to a quantum quench conditioned on the state of the qubit being $|\uparrow\rangle$. The quench is triggered by applying a Hadamard gate (denoted H) to the qubit, which, after undergoing free evolution while in contact with the magnon mode, is then measured in the X basis.

Phase-estimation protocol—The qubit is prepared in $|\downarrow\rangle$, and the magnon mode is allowed to equilibrate in contact with the qubit, eventually settling into its ground state $|0\rangle_{\downarrow}$. Since $|0\rangle_{\downarrow}$ is a squeezed state of the α_{\uparrow} mode [cf. Eq. (5)], the squeezed magnons become real (on-shell) as soon as the state of the qubit is flipped to $|\uparrow\rangle$. These squeezed magnons can then be used to estimate the eigen-mode frequency ω_{\uparrow} with Heisenberg-limited precision. To estimate ω_{\downarrow} , the qubit could instead be initialized in $|\uparrow\rangle$ so that the magnon mode is prepared in $|0\rangle_{\uparrow}$. The use of equilibrium, ground-state squeezing is a unique feature of this quantum-metrology protocol relative to schemes based on photonic and atomic-spin squeezing, and also relative to the cavity-magnonic scheme of Ref. [43], where entanglement between the cavity and magnon mode generated for the purpose of measuring the magnon via the cavity may in certain situations adversely affect the usefulness of magnon squeezing in achieving sub-SQL precision.

Following the preparation of the magnon mode in $|0\rangle_{\downarrow}$, the remainder of the protocol is as follows: At time $t = 0$, a Hadamard gate (denoted H in Fig. 2) is applied to the qubit to prepare the state $|+\rangle = (|\uparrow\rangle + |\downarrow\rangle)/\sqrt{2}$. As a result of this Hadamard, the magnon mode will experience a qubit-conditioned quantum quench: For a qubit in state $|\downarrow\rangle$, evolution is generated by H_{\downarrow} and the magnon mode remains in its ground state, while for a qubit in state $|\uparrow\rangle$, evolution is instead generated by H_{\uparrow} , for which $|0\rangle_{\downarrow}$ is no longer an eigenstate [cf. Eq. (5)]. The unitary U describing the evolution of the coupled qubit-magnon system can therefore be written as

$$U = |\downarrow\rangle\langle\downarrow| \otimes U_{\downarrow} + |\uparrow\rangle\langle\uparrow| \otimes U_{\uparrow}, \quad (6)$$

where $U_{\sigma} = e^{-iH_{\sigma}t}$. For a magnon mode initialized in $|0\rangle_{\downarrow}$, the $|\downarrow\rangle$ -conditioned evolution generated by H_{\downarrow} acts trivially: $U_{\downarrow}|0\rangle_{\downarrow} = |0\rangle_{\downarrow}$ (Fig. 2).

Following the Hadamard, the qubit and magnon mode are allowed to evolve under the action of U [Eq. (6)].

The qubit is then measured in the X basis $|\pm\rangle$, yielding the expectation value $\langle\sigma_x\rangle = \text{Tr}\{U\rho_0U^{\dagger}\sigma_x\}$, where $\rho_0 = |\psi_0\rangle\langle\psi_0|$ for $|\psi_0\rangle = |+\rangle \otimes |0\rangle_{\downarrow}$. For a total evolution time t , this expectation value can be written as

$$\langle\sigma_x\rangle_t = \text{Re}_{\downarrow}\langle 0|U_{\uparrow}(t)|0\rangle_{\downarrow}, \quad (7)$$

where $\downarrow\langle 0|U_{\uparrow}(t)|0\rangle_{\downarrow}$ is the dynamical overlap of the initial state $|0\rangle_{\downarrow}$ with the time-evolved state $U_{\uparrow}|0\rangle_{\downarrow}$. Since $|0\rangle_{\downarrow}$ contains only even Fock states of the α_{\uparrow} mode [cf. Eq. (5)], this overlap is periodic in π/ω_{\uparrow} . As a function of time, $\langle\sigma_x\rangle_t$ will therefore exhibit periodic collapses and recurrences occurring at multiples of π/ω_{\uparrow} , which become increasingly localized as the relative squeezing strength $r = r_{\downarrow} - r_{\uparrow}$ is increased (Fig. 3). This can be understood through the lens of the orthogonality catastrophe as being a consequence of the magnon mode having a quantum speed limit that scales extensively with the average mode occupation [44]: For this protocol, the magnitude $|\langle\sigma_x\rangle_t| = (1/2)\cos\Theta(t)$ of the qubit coherence $\sigma_{+} = (\sigma_x + i\sigma_y)/2$ is related to the Bures angle $\Theta(t) = \arccos|\downarrow\langle 0|U_{\uparrow}(t)|0\rangle_{\downarrow}|$ between $|0\rangle_{\downarrow}$ and $U_{\uparrow}|0\rangle_{\downarrow}$. For all times t , $\Theta(t)$ is bounded by the quantum speed limit v_{QSL} according to $\Theta(t) \leq \int_0^t dt' v_{\text{QSL}}(t')$ [45, 46], where $v_{\text{QSL}} = \sqrt{F_{\text{Q}}}/2$ depends on the quantum Fisher information F_{Q} with respect to time of the instantaneous state [46]. For Hamiltonian evolution, F_{Q} is constant and given by four times the variance of the generator of time evolution with respect to the initial state, which in our case, corresponds to $F_{\text{Q}} = 4\text{Var}_{|0\rangle_{\downarrow}}(H_{\uparrow}) = 8\omega_{\uparrow}^2(\bar{n}^2 + \bar{n})$, where here, $\bar{n} = \sinh^2 r$ is the average number of magnons in the squeezed state of the α_{\uparrow} mode. The post-quench recurrences in the qubit coherence therefore become increasingly localized as the squeezing parameter r is increased. These localized recurrences are ultimately what we use to estimate ω_{\uparrow} , but we remark that the non-classicality of the magnon state has not yet played a role: Classical coherent-state overlaps of the form $\langle\alpha|e^{-i\omega t}\alpha\rangle$ would exhibit qualitatively similar collapses and recurrences since the quantum speed limit relevant to this scenario also scales extensively with the number of particles $\bar{n} = |\alpha|^2$. However, the real, squeezed magnons produced by the quench do enable parameter estimation with a precision exceeding that allowed by classical resources.

Heisenberg-limited scaling near the post-quench recurrences—For the X-basis measurement of the qubit, the probability $p(+|\phi)$ of measuring the qubit in state $|+\rangle$ given some value of $\phi = \omega_{\uparrow}t$ follows from Eqs. (5) and (7) and is given by

$$p(+|\phi) = \frac{1}{2} + \frac{1}{2} \sum_n |c_{2n}(r)|^2 \cos(2n\phi). \quad (8)$$

The Heisenberg-limited scaling enabled by this protocol in the vicinity of a qubit-coherence recurrence (occurring at times t such that $\phi = m\pi$ with $m \in \mathbb{Z}$) ultimately

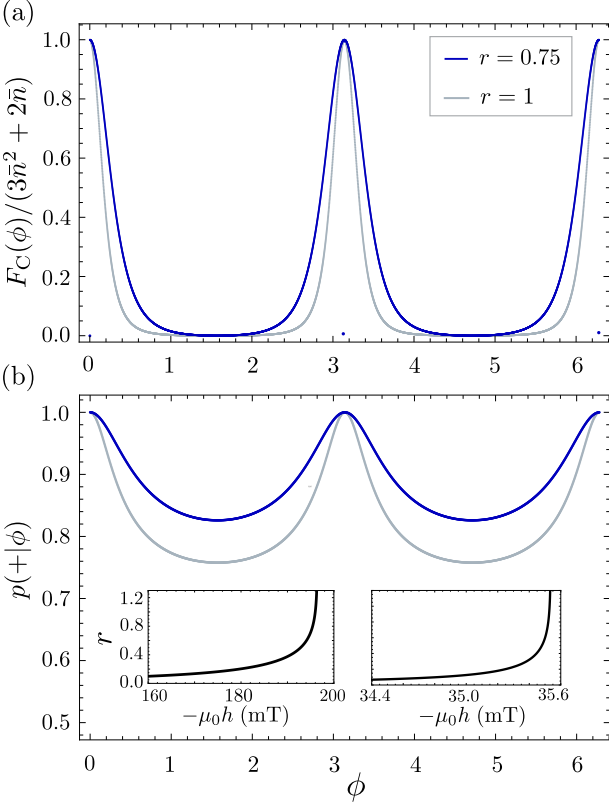


FIG. 3. (a) Fisher information $F_C(\phi)$ evaluated using Eqs. (8) and (10) for $r = 0.75$ (dark blue) and $r = 1$ (light blue). As described in the text, the duration T of the free-evolution window should be chosen so that $\phi = \omega_{\uparrow}T$ is approximately equal to $m\pi$. The free-evolution time T could be tweaked adaptively using the tunability of the squeezing parameter as a function of the applied magnetic field. (b) Probability $p(+|\phi = \omega_{\uparrow}t) = (1/2)(1 + \langle \sigma_x \rangle_t)$ of measuring the qubit in the state $|+\rangle$ given a value of ϕ . In the absence of ground-state squeezing ($\Omega = 0$, corresponding to $r_{\uparrow} = r_{\downarrow} = r = 0$), the probability is $p(+|\phi) = 1$ independent of ϕ , and the Fisher information associated with the measurement is zero. Left inset: Squeezing parameter r as a function of the applied magnetic field h for $(2SK_z - SK_y)/2\pi = 7$ GHz and $\Omega/2\pi = \chi/2\pi = 0.5$ GHz. A field of 180 mT corresponds to a Zeeman splitting of 5.04 GHz (assuming a g-factor of 2). Right inset: The same range of squeezing parameters could be achieved with the same value of $\Omega/2\pi = 0.5$ GHz, $(2SK_z - SK_y)/2\pi = 2$ GHz, and a considerably smaller dispersive coupling of $\chi/2\pi = 5$ MHz [10].

arises from super-resolution $\phi \mapsto 2n\phi$ [40] of the parameter ϕ in Eq. (8), as we now show by calculating the Fisher information associated with the qubit measurement.

The best precision that can be achieved with M independent measurements and an unbiased estimator of ϕ is given by the Cramér-Rao bound [47],

$$\delta\phi^2 \geq \frac{1}{MF_C(\phi)}, \quad (9)$$

where here, $F_C(\phi)$ is the Fisher information quantifying

the amount of information about ϕ that can be extracted from the probability distribution describing the measurement outcomes. For a binary measurement like the X-basis qubit measurement considered here,

$$F_C(\phi) = \sum_{x=\pm} p(x|\phi) [\partial_{\phi} \ln p(x|\phi)]^2. \quad (10)$$

This quantity can be evaluated using the expression for $p(+|\phi)$ given in Eq. (8). Exactly at $\phi = m\pi$ ($m \in \mathbb{Z}$), the Fisher information vanishes since $\partial_{\phi} p(+|\phi)|_{m\pi} = 0$. For $\phi \neq m\pi$ and $|\phi - m\pi| \ll \bar{n}^{-1}$ with $\bar{n} \gtrsim 1$, we can expand the trigonometric functions to leading nontrivial order in ϕ , giving $F_C(\phi) \simeq \sum_n |c_{2n}|^2 (2n)^2$. This sum is equal to the average of $(\alpha_{\uparrow}^{\dagger} \alpha_{\uparrow})^2$ with respect to $|0\rangle_{\downarrow}$ [cf. Eq. (5)]. Using Wick's theorem, this average can be rewritten entirely in terms of the expectation values $\langle \downarrow | \alpha_{\uparrow}^2 | 0 \rangle_{\downarrow} = -(1/2) \sinh(2r)$ and $\langle \downarrow | \alpha_{\uparrow}^{\dagger} \alpha_{\uparrow} | 0 \rangle_{\downarrow} = \sinh^2 r$, giving

$$F_C(\phi) \simeq 3\bar{n}^2 + 2\bar{n}, \quad 0 < |\phi - m\pi| \ll \bar{n}^{-1}, \quad \bar{n} \gtrsim 1, \quad (11)$$

where $\bar{n} = \sinh^2 r$ is the average number of real magnons produced by the quantum quench. The Heisenberg scaling \bar{n}^2 in Eq. (11) is the main result of this work. Since $\bar{n} = 0$ in the absence of squeezing terms $\propto \Omega$ in H_0 [Eq. (2)], the parameter estimation enabled by this protocol is due entirely to the quantum features of the magnon state. Although Eq. (11) gives the scaling of $F_C(\phi)$ with \bar{n} for $\bar{n} \gtrsim 1$, the fact that $F_C(\phi) = 0$ for $\bar{n} = \sinh^2 r = 0$ follows directly from the fact that for $r = 0$, we have $p(+|\phi) = 1$ independent of ϕ .

Away from the regime $0 < |\phi - m\pi| \ll \bar{n}^{-1}$, $F_C(\phi)$ can be evaluated numerically [Fig. 3(a)]. Since maximum-likelihood estimation saturates the Cramér-Rao bound in the limit of many measurements [47], Heisenberg-limited estimation of the magnon-mode frequency ω_{\uparrow} can be achieved by performing maximum likelihood estimation of ϕ based on the probability distribution $p(+|\phi)$ in the vicinity of any post-quench recurrence of the qubit coherence [Fig. 3(b)]. Concretely, the protocol would require timing the total duration T of the free-evolution window so that ϕ is close to $m\pi$, where the dependence of the qubit-measurement outcomes is strongly dependent on ϕ . This tuning of T could be performed adaptively by controlling the squeezing parameter r via the external magnetic field h [Fig. 3(b,inset)], beginning with a low value of r and increasing it as the location of the periodic recurrences is revealed. Then, given some sequence $\mathbf{x} = \{x_1, \dots, x_M\}$ of M measurement outcomes ($x_i = \pm$) each resulting from measurement at time $t = T$, the maximum-likelihood estimator ϕ_{MLE} can be written as $\phi_{\text{MLE}}(\mathbf{x}) = \text{argmax}_{\phi} \prod_{i=1}^M p(x_i|\phi)$. In the limit of large M , it will approach a Gaussian centered at the true value of ϕ with a variance equal to the inverse of $MF_C(\phi)$: $P(\phi_{\text{MLE}}|\phi) = \sqrt{MF_C(\phi)/2\pi} e^{-[MF_C(\phi)/2](\phi - \phi_{\text{MLE}})^2}$ [48].

Effects of qubit dephasing—To calculate the effects of (quasistatic) qubit dephasing on the Fisher information

F_C , we now include in H_0 an additional term $\eta\sigma_z/2$, where η is a zero-mean, Gaussian random variable with $\langle\eta\rangle = 0$ and $\langle\eta^2\rangle = 2/T_2^*$. Here, T_2^* is the qubit dephasing time and $\langle\cdot\rangle$ denotes an average over the probability distribution $p(\eta)$ governing the distribution of η -values from one shot to the next: $\langle\cdot\rangle = \int d\eta p(\eta)\langle\cdot\rangle$. For a fixed value of η , $\langle\sigma_x\rangle_t = (1/2)e^{i\eta t}\langle 0|U_\uparrow|0\rangle_\downarrow + \text{c.c.}$, giving

$$\langle\langle\langle\sigma_x\rangle_t\rangle\rangle = e^{-(t/T_2^*)^2} \text{Re}_\downarrow\langle 0|U_\uparrow(t)|0\rangle_\downarrow. \quad (12)$$

Expanding as before about $\phi = m\pi$, we find that in the presence of qubit dephasing, the local maxima in the Fisher information will be modified by a decaying Gaussian envelope according to

$$F_C(\phi) \simeq e^{-(Km)^2} (3\bar{n}^2 + 2\bar{n}), \quad (13)$$

valid for $0 < |\phi - m\pi| \ll \bar{n}^{-1}$. Here, we have introduced a dimensionless parameter $K = \pi/(\omega_\uparrow T_2^*)$ controlling the decay of the m^{th} recurrence relative to the ideal case where $T_2^* \rightarrow \infty$. In the left inset of Fig. 3(b), we plot the squeezing parameter $r = r_\downarrow - r_\uparrow$ as a function of the applied magnetic field $\mu_0 h$ in mT, with $\omega_0/2\pi = (7 + |\gamma| \mu_0 h)$ GHz and $\chi/2\pi = \Omega/2\pi = 0.5$ GHz chosen so that the range of applied magnetic fields over which $r \approx 1$ gives Zeeman splittings of approximately 5 GHz, assuming a g-factor of 2. With these parameters, $\omega_\uparrow/2\pi = 2.8$ GHz for $r = 1$. Hence, provided T_2^* exceeds a tenth of a nanosecond, qubit dephasing should not present a limiting error source for this protocol since $\omega_\uparrow T_2^* \gg 1$ for such T_2^* . In the right inset of Fig. 3(b), we assume a much smaller dispersive coupling of $\chi/2\pi = 5$ MHz, as has recently been realized for cavity-mediated coupling between a superconducting transmon qubit and yttrium iron garnet (YIG) sphere [10]. In this case, the same range of squeezing strengths could be realized with $\Omega/2\pi = 0.5$ GHz and $\omega_0/2\pi = (2 + |\gamma| \mu_0 h)$ GHz.

Conclusion—We have presented a measurement protocol enabling Heisenberg-limited metrology with equilibrium ground-state squeezing in magnetic systems. Dispersive coupling to a qubit can be used to subject the magnon mode to a quantum quench conditioned on the state of the qubit. This quench produces real squeezed magnons in a process that may be viewed as a magnon analog of the dynamical Casimir effect. The interaction of the qubit with the magnon system then manifests as super-resolution of an unknown parameter in the qubit coherence, enabling precision beyond the SQL. In the future, the protocol presented here could pave the way for new approaches that seek to harness the quantum properties of magnetic ground states for tasks beyond the reach of classical resources.

Acknowledgments—ZMM thanks W. A. Coish for useful discussions. This work was supported by the Georg H. Endress Foundation and by the Swiss National Science Foundation, NCCR SPIN (Grant No. 51NF40-180604).

* zoe.mcintyre@unibas.ch

† ji.zou@unibas.ch

- [1] P. Kok, W. J. Munro, K. Nemoto, T. C. Ralph, J. P. Dowling, and G. J. Milburn, Linear optical quantum computing with photonic qubits, *Rev. Mod. Phys.* **79**, 135 (2007).
- [2] M. Aspelmeyer, T. J. Kippenberg, and F. Marquardt, Cavity optomechanics, *Rev. Mod. Phys.* **86**, 1391 (2014).
- [3] H. Y. Yuan, Y. Cao, A. Kamra, R. A. Duine, and P. Yan, Quantum magnonics: When magnon spintronics meets quantum information science, *Physics Reports* **965**, 1 (2022).
- [4] A. V. Chumak, P. Kabos, M. Wu, C. Abert, C. Adelmann, A. O. Adeyeye, J. Åkerman, F. G. Aliev, A. Anane, A. Awad, *et al.*, Advances in magnetics roadmap on spin-wave computing, *IEEE Trans. Magn.* **58**, 1 (2022).
- [5] Q. Wang, G. Csaba, R. Verba, A. V. Chumak, and P. Pirro, Nanoscale magnonic networks, *Phys. Rev. Appl.* **21**, 040503 (2024).
- [6] Y. Tabuchi, S. Ishino, A. Noguchi, T. Ishikawa, R. Yamazaki, K. Usami, and Y. Nakamura, Coherent coupling between a ferromagnetic magnon and a superconducting qubit, *Science* **349**, 405 (2015).
- [7] D. Lachance-Quirion, Y. Tabuchi, S. Ishino, A. Noguchi, T. Ishikawa, R. Yamazaki, and Y. Nakamura, Resolving quanta of collective spin excitations in a millimeter-sized ferromagnet, *Sci. Adv.* **3**, e1603150 (2017).
- [8] D. Lachance-Quirion, S. P. Wolski, Y. Tabuchi, S. Kono, K. Usami, and Y. Nakamura, Entanglement-based single-shot detection of a single magnon with a superconducting qubit, *Science* **367**, 425 (2020).
- [9] D. Xu, X.-K. Gu, H.-K. Li, Y.-C. Weng, Y.-P. Wang, J. Li, H. Wang, S.-Y. Zhu, and J. You, Quantum control of a single magnon in a macroscopic spin system, *Phys. Rev. Lett.* **130**, 193603 (2023).
- [10] J. Q. You, Y.-C. Weng, D. Xu, Z. Chen, L.-Z. Tan, X.-K. Gu, J. Li, H.-F. Yu, S. Zhu, X. Hu, *et al.*, Quantum nonlinear magnonics: Magnon squeezing in the quantum regime, <http://dx.doi.org/10.21203/rs.3.rs-6757664/v1> (2025).
- [11] D. F. Walls, Squeezed states of light, *Nature* **306**, 141 (1983).
- [12] V. Giovannetti, S. Lloyd, and L. Maccone, Quantum metrology, *Phys. Rev. Lett.* **96**, 010401 (2006).
- [13] C. M. Caves, Quantum-mechanical noise in an interferometer, *Phys. Rev. D* **23**, 1693 (1981).
- [14] M. D. Lang and C. M. Caves, Optimal quantum-enhanced interferometry using a laser power source, *Phys. Rev. Lett.* **111**, 173601 (2013).
- [15] L. Pezzé and A. Smerzi, Mach-Zehnder interferometry at the Heisenberg limit with coherent and squeezed-vacuum light, *Phys. Rev. Lett.* **100**, 073601 (2008).
- [16] J. A. H. Nielsen, J. S. Neergaard-Nielsen, T. Gehring, and U. L. Andersen, Deterministic quantum phase estimation beyond N00N states, *Phys. Rev. Lett.* **130**, 123603 (2023).
- [17] M. Tse, H. Yu, N. Kijbunchoo, A. Fernandez-Galiana, P. Dupej, L. Barsotti, C. D. Blair, D. D. Brown, S. E. e. Dwyer, A. Effler, *et al.*, Quantum-enhanced advanced LIGO detectors in the era of gravitational-wave astron-

- omy, Phys. Rev. Lett. **123**, 231107 (2019).
- [18] M. Kitagawa and M. Ueda, Squeezed spin states, Phys. Rev. A **47**, 5138 (1993).
- [19] D. J. Wineland, J. J. Bollinger, W. M. Itano, and D. J. Heinzen, Squeezed atomic states and projection noise in spectroscopy, Phys. Rev. A **50**, 67 (1994).
- [20] C. Gross, Spin squeezing, entanglement and quantum metrology with Bose–Einstein condensates, J. Phys. B: At. Mol. Opt. Phys. **45**, 103001 (2012).
- [21] L. Pezze, A. Smerzi, M. K. Oberthaler, R. Schmied, and P. Treutlein, Quantum metrology with nonclassical states of atomic ensembles, Reviews of Modern Physics **90**, 035005 (2018).
- [22] A. Sørensen, L.-M. Duan, J. I. Cirac, and P. Zoller, Many-particle entanglement with Bose–Einstein condensates, Nature **409**, 63 (2001).
- [23] C. Gross, T. Zibold, E. Nicklas, J. Esteve, and M. K. Oberthaler, Nonlinear atom interferometer surpasses classical precision limit, Nature **464**, 1165 (2010).
- [24] A. S. Sørensen and K. Mølmer, Entangling atoms in bad cavities, Phys. Rev. A **66**, 022314 (2002).
- [25] L.-A. Wu, H. J. Kimble, J. L. Hall, and H. Wu, Generation of squeezed states by parametric down conversion, Phys. Rev. Lett. **57**, 2520 (1986).
- [26] A. Kamra and W. Belzig, Super-Poissonian shot noise of squeezed-magnon mediated spin transport, Phys. Rev. Lett. **116**, 146601 (2016).
- [27] A. Kamra and W. Belzig, Magnon-mediated spin current noise in ferromagnet–nonmagnetic conductor hybrids, Phys. Rev. B **94**, 014419 (2016).
- [28] J. Zou, S. K. Kim, and Y. Tserkovnyak, Tuning entanglement by squeezing magnons in anisotropic magnets, Phys. Rev. B **101**, 014416 (2020).
- [29] A. Kamra, E. Thingstad, G. Rastelli, R. A. Duine, A. Brataas, W. Belzig, and A. Sudbø, Antiferromagnetic magnons as highly squeezed Fock states underlying quantum correlations, Phys. Rev. B **100**, 174407 (2019).
- [30] A. Kamra, W. Belzig, and A. Brataas, Magnon-squeezing as a niche of quantum magnonics, Appl. Phys. Lett. **117** (2020).
- [31] A.-L. E. Römling, A. Vivas-Viaña, C. S. Muñoz, and A. Kamra, Resolving nonclassical magnon composition of a magnetic ground state via a qubit, Phys. Rev. Lett. **131**, 143602 (2023).
- [32] A.-L. E. Römling and A. Kamra, Quantum sensing of antiferromagnetic magnon two-mode squeezed vacuum, Phys. Rev. B **109**, 174410 (2024).
- [33] M. Eaton, A. Hossameldin, R. J. Birrittella, P. M. Alsing, C. C. Gerry, H. Dong, C. Cuevas, and O. Pfister, Resolution of 100 photons and quantum generation of unbiased random numbers, Nat. Photon. **17**, 106 (2023).
- [34] P. M. Anisimov, G. M. Raterman, A. Chiruvelli, W. N. Plick, S. D. Huver, H. Lee, and J. P. Dowling, Quantum metrology with two-mode squeezed vacuum: Parity detection beats the Heisenberg limit, Phys. Rev. Lett. **104**, 103602 (2010).
- [35] K. P. Seshadreesan, P. M. Anisimov, H. Lee, and J. P. Dowling, Parity detection achieves the Heisenberg limit in interferometry with coherent mixed with squeezed vacuum light, New J. Phys. **13**, 083026 (2011).
- [36] B. T. Gard, C. You, D. K. Mishra, R. Singh, H. Lee, T. R. Corbitt, and J. P. Dowling, Nearly optimal measurement schemes in a noisy Mach–Zehnder interferometer with coherent and squeezed vacuum, EPJ Quantum Technol. **4**, 1 (2017).
- [37] Z. M. McIntyre and W. A. Coish, Homodyne detection is optimal for quantum interferometry with path-entangled coherent states, Phys. Rev. A **110**, L010602 (2024).
- [38] C. Gross, H. Strobel, E. Nicklas, T. Zibold, N. Barrigill, G. Kurizki, and M. K. Oberthaler, Atomic homodyne detection of continuous-variable entangled twin-atom states, Nature **480**, 219 (2011).
- [39] V. Dodonov, Fifty years of the dynamical Casimir effect, Physics **2**, 67 (2020).
- [40] K. J. Resch, K. L. Pregnell, R. Prevedel, A. Gilchrist, G. J. Pryde, J. L. O’Brien, and A. G. White, Time-reversal and super-resolving phase measurements, Phys. Rev. Lett. **98**, 223601 (2007).
- [41] I. C. Skogvoll, J. Lidal, J. Danon, and A. Kamra, Tunable anisotropic quantum Rabi model via a magnon–spin-qubit ensemble, Phys. Rev. Appl. **16**, 064008 (2021).
- [42] C. C. Gerry and P. L. Knight, *Introductory quantum optics* (Cambridge University Press, 2023).
- [43] Q.-K. Wan, H.-L. Shi, and X.-W. Guan, Quantum-enhanced metrology in cavity magnonics, Phys. Rev. B **109**, L041301 (2024).
- [44] T. Fogarty, S. Deffner, T. Busch, and S. Campbell, Orthogonality catastrophe as a consequence of the quantum speed limit, Phys. Rev. Lett. **124**, 110601 (2020).
- [45] W. K. Wootters, Statistical distance and Hilbert space, Phys. Rev. D **23**, 357 (1981).
- [46] M. M. Taddei, B. M. Escher, L. Davidovich, and R. L. de Matos Filho, Quantum speed limit for physical processes, Phys. Rev. Lett. **110**, 050402 (2013).
- [47] H. Cramér, *Mathematical methods of statistics*, Vol. 9 (Princeton University Press, 1999).
- [48] E. L. Lehmann and G. Casella, *Theory of Point Estimation* (Springer, 1998).